NMR Study of L-Shaped (Quinoxaline)platinum(II) Complexes − Crystal Structure of $[Pt(DMeDPQ)(bipy)](PF_6)_2$

Enrico Rotondo,*[a] Archimede Rotondo,[a] Francesco Nicolò,[a] Maria Letizia Di Pietro,[a] Maria Anna Messina,[a] and Matteo Cusumano[a]

Keywords: DNA recognition / N ligands / Nitrogen heterocycles / NMR spectroscopy / Platinum

A ^1H and ^{13}C NMR study of nine Pt^{II} complexes of DMeDPQ [6,7-dimethyl-2,3-bis(2-pyridyl)quinoxaline] and BDPQ [2,3-bis(2-pyridyl)benzo[*g*]quinoxaline], and the crystal structure of one of them, are reported. The results are consistent with C_s symmetry of "L-shaped square-planar complexes". The rigid seven-membered chelated quinoxaline ligand holds the fused aromatic rings nearly perpendicular to the Pt^{II} coordination plane, generating the peculiar L-shaped structure. Ancillary ligands in the residual coordination sites are: a) bidentate flexible-planar 2,2′-bipyridine (bipy; complexes **1** and **2**); b) bidentate rigid-planar dipyrido[3,2-*a*:2′3′-*c*]phenazine (dppz) or benzo[*b*]dipyrido[3,2-*h*:2′,3′-*j*]phenazine (bdppz; complexes **3**–**6**); or c) 3-substituted monodentate pyridines (3-Rpy; complexes **7**–**9**). The L-shaped geometry has been exploited to gain insight into the steric and dynamic features that regulate the noncovalent interactions of these square-planar complexes with DNA. We have shown previously, for $[Pt(bipy)(n\text{-}Rpy)_2]^{2+}$, that bipy twisting can be frozen out on the NMR timescale below 260 K. Preservation of the C_s symmetry at low temperature indicates a lack of bipy fluxionality within these L-shaped structures. The static butterfly-like symmetric orientation of the quinoxaline pyridyl rings accounts for the hampered twisting of Pt(bipy), which is otherwise assisted by the synchronous "windscreen wiper" conrotatory rocking of the ancillary pyridine rings. The L-geometry can also be used to monitor the ancillary *n*-Rpy rotation by NMR spectroscopy. The quasi-vertical quinoxaline pyridyl rings alignment leave room in the coordination plane for the crossing of the opposite pyridine rings, thereby reducing their rotational barriers about the Pt–N bond.

Introduction

In the course of our interest in intercalative, noncovalent interaction of square-planar Pt^{II} complexes with DNA duplex, we have recently synthesised platinum(II) complexes of DMeDPQ and BDPQ. These ligands display a rather flexible metal-ion binding pattern often characterised by chelation through the pyrazine and pyridyl nitrogen atoms to form potentially dicompartmental five-membered ring ligands. Different coordination patterns, however, are also known. On the basis of literature reports three main coordination geometries can be envisaged for these ligands: (i) half-filled mononuclear;[1] (ii) completely filled dinuclear (the ligand acts as a two-metal bridge);[2] and (iii) a less-common seven-membered bis(pyridyl)metal chelate ring[3] (Scheme 1). One case of BDPQ three-coordination through two pyridyl nitrogen atoms and the deprotonated hydroxy oxygen atom of the hydrate ligand has also been reported.[4]

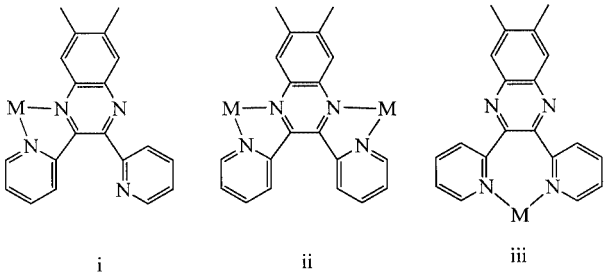

i ii iii

Scheme 1. Common coordination modes adopted by BDPQ and DMeDPQ

Most of the known DMeDPQ and BDPQ complexes were unambiguously characterised by X-ray crystallography as mononuclear and binuclear octahedral complexes, and very few tetracoordinate complexes have been reported so far.[5] We have recently found that in $[PdCl_2(DMeDPQ)]$[6] and $[Pt(BDPQ)(bipy)](PF_6)_2$ [7] the quinoxalines coordinate to the metal as seven-membered bis-pyridyl chelates. This binding holds the fused aromatic rings perpendicular to the coordination plane to give an angular "L-shaped" structure (Figure 1).

The same coordination geometry has been reported for $[PtCl_2(DMeDPQ)]$[8] and $[Pd(DPQ)_2](PF_6)_2$.[9] Saturation of

[a] Dipartimento di Chimica Inorganica, Chimica Analitica e Chimica Fisica, Facoltà di Scienze, Università di Messina
Salita Sperone 31, 98166 Messina, Italy
Fax: + 39-090-393-756
E-mail: rotondo@chem.unime.it

  DOI: 10.1002/ejic.200400421

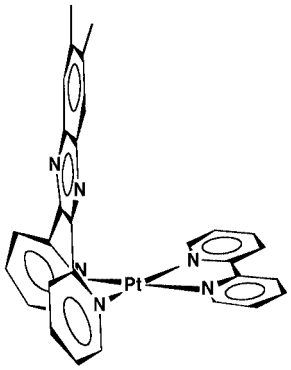

Figure 1. Schematic drawing of $[Pt(DMeDPQ)(bipy)]^{2+}$

the residual coordination sites of (quinoxaline)Pt^{II} substrates with flat bidentate ligands led to the six mixed complexes **1**−**6**, which bear two extended mutually orthogonal planar moieties, both of which are capable of undergoing intercalation as well as enantioselective DNA recognition. The ambintercalating character of these complexes has been investigated recently.[7] In this paper we report the ^1H and ^{13}C NMR spectroscopic characterisation of the ambintercalator complexes **1**−**6**, and their monodentate pyridine analogues **7**−**9** (see Scheme 2). The crystal structure of $[Pt(DMeDPQ)(bipy)](PF_6)_2$ (**1**) has also been resolved by X-ray diffraction. The unambiguous resonance assignment and structure determination are essential steps on the way toward intercalative mapping driven by magnetic perturbation of the nuclei upon insertion into the DNA double helix. Moreover, we designed the quinoxaline coordination geometry to gain insight into the structural and dynamic features regulating the noncovalent interactions of the square-planar complexes with DNA. Despite quinoxalines' versatility to act as a magnetic probe of the structural and dynamic features of the ancillary ligands, NMR studies of these L-shaped Pt^{II} complexes have, up to now, been largely neglected.

Results and Discussion

The syntheses of complexes **1**−**9** are discribed in the Exp. Sect.

Our experimental evidence is consistent with DMeDPQ and BDPQ acting as bidentate seven-membered dipyridyl chelates. The ancillary ligands in the residual coordination sites of the nine complexes studied here belong to three different classes: a) bidentate-planar with a certain degree of flexibility (bipy; complexes **1** and **2**); b) more rigid bidentate-planar phenazine (dppz and bdppz; complexes **3**−**6**); c) monodentate pyridines (3-Rpy, R = H, CH_3; complexes **7**−**9**). 2-D representations of the ligands and schematic formulae for complexes **1**−**9** are given in Scheme 2.

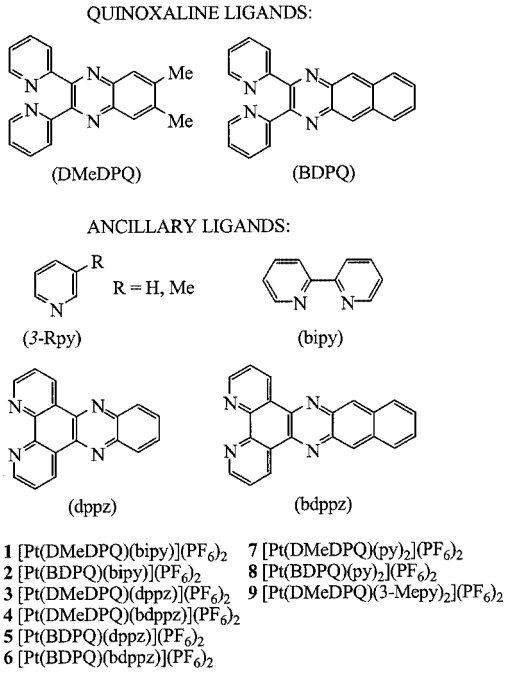

Scheme 2. 2D representation of ligands and schematic formulae **1**−**9**

The solid-state structure, solved by X-ray diffraction, unequivocally shows the L-shaped nature of **1**. The same coordination has previously been found for analogous substrates,[6−9] meaning that "L-shaped" is the preferred structure for square-planar (quinoxaline)Pt^{II} and -Pd^{II} complexes. This geometry has C_s symmetry due to a vertical mirror plane (σ_v) intersecting the metal atom. The high-resolution NMR spectra are consistent with this symmetry element, as single signals are detected for every pair of nuclei interchanged by the symmetry operation. Standard 1- and 2-D NMR techniques were employed for thorough resonance assignment (Tables 1 and 2).

Discrimination between the quinoxaline pyridyl and the 2,2′-bipyridine proton resonances of **1** and **2** was achieved by heteronuclear long-range C-7′/3′-H coupling, which allowed the assignment of 3′-H and thus the whole set of pyridyl resonances. Analogously, the phenazine pyridyl resonances could be assigned due to the heteronuclear long-range C-7/4-H coupling (C-7 signal at higher field than C-7′ signal). Together with other data, dipolar 10-H/4-H coupling of the planar phenazine protons, which is not found between 10′-H and 3′-H or 10′-H and 4′-H of the bent quinoxaline, confirmed the heteronuclear long-range coupling assignments of **3**−**6**. A peculiar, previously reported ^1H NMR spectral feature of $[Pt(bipy)(n\text{-}Rpy)_2]^{2+}$ is a strong diamagnetic shift experienced by the 6-H protons of the bipy ligand because of the anisotropic ring current of the quasi-perpendicular *n*-Rpy group.[10] We found a similar effect in **1** and **2**, where the seven-membered chelates hold the bis(pyridyl) vertical rings just above 6-H of bipy. This diamagnetic shift is less in rigidly planar phenazine complexes **3**−**6**, and even more so in the 3-Rpy derivatives **7**−**9**.

Table 1. Selected ^{1}H NMR resonances of complexes **1**−**9** in [D$_6$]acetone at 298 K

	2-H	3-H	4-H	5-H	6-H	10-H	11-H	12-H	13-H	3′-H	4′-H	5′-H	6′-H	10′-H	12′-H	13′-H
1	–	8.67	8.53	7.83	8.18	–	–	–	–	8.29	8.57	8.14	9.46	8.05	2.58	–
2	–	8.65	8.53	7.85	8.22	–	–	–	–	8.39	8.61	8.18	9.52	8.98	8.34	7.78
3	–	–	10.01	8.33	8.71	8.47	8.21	–	–	8.36	8.63	8.21	9.60	8.05	2.54	–
4	–	–	9.88	8.29	8.65	8.92	–	8.14	7.55	8.39	8.65	8.23	9.62	8.09	2.54	–
5	–	–	9.99	8.33	8.73	8.43	8.17	–		8.45	8.66	8.29	9.65	8.96	8.31	7.73
6	–	–	9.86	8.29	8.66	8.88	–	8.11	7.52	8.48	8.68	8.29	9.67	9.00	8.29	7.71
7	8.92	7.62	8.07	7.62	8.92	–	–	–	–	8.21	8.37	7.86	9.24	8.19	2.70	–
8	8.94	7.62	8.07	7.62	8.94	–	–	–	–	8.31	8.40	7.91	9.29	9.12	8.46	7.88
9	8.80	–	7.86	7.47	8.71					8.19	8.35	7.86	9.22	8.20	2.70	–

Table 2. Selected ^{13}C{^{1}H} NMR resonances of complexes **1**−**9** in [D$_6$]acetone at 298 K

	C-2	C-3	C-4	C-5	C-6	C-7	C-2′	C-3′	C-4′	C-5′	C-6′	C-7′	C-9′	C-10′
1	157.5	125.6	143.7	129.8	150.9	–	158.8	131.0	143.9	130.2	153.2	147.4	145.2	129.2
2	157.6	125.6	143.9	129.8	150.9	–	158.6	131.3	144.0	130.4	153.3	148.7	138.4	129.6
3	151.1	131.7	139.5	129.3	152.9	143.7	159.0	131.2	143.9	130.3	153.4	147.6	145.5	129.2
4	151.5	131.8	139.4	129.6	152.9	140.0	159.0	131.2	144.0	130.4	153.5	147.6	145.6	129.1
5	151.1	131.6	139.5	129.5	152.9	143.7	158.8	131.4	144.1	130.6	153.5	148.6	138.3	129.3
6	151.4	131.8	139.4	129.5	152.9	140.0	158.8	131.5	144.1	130.6	153.6	148.6	138.4	129.5
7	152.7	128.8	142.5	128.8	152.7	–	158.6	130.9	143.2	128.9	152.1	147.6	145.2	129.5
8	152.7	128.8	142.6	128.8	152.7	–	158.5	131.1	143.4	129.1	152.3	148.7	138.9	129.7
9	152.0	139.2	142.6	127.7	149.5	17.9	158.3	130.5	142.9	128.5	151.8	147.5	145.2	129.3

Coordinated bipy is usually thought of as a perfectly flat fragment; however, we have previously proposed a slight propeller-like torsion of the ligand in [Pt(bipy)(*n*-Rpy)$_2$]$^{2+}$ cations on the basis of both low-temperature NMR spectra[10] and X-ray crystal structures.[11] Indeed, in order to minimize intramolecular bumping, these complexes undergo a slight bipy-propeller distortion concerted to an about 10° conrotation of the quasi-vertical *n*-Rpy. NMR spectra consistent with time-averaged C_{2v} symmetry are due to fast bipy twisting synchronous to windscreen wiper rocking of *n*-Rpy. Locked propeller structures can be witnessed by low-temperature resonance splitting observed for nonfluxional molecules devoid of C_2 symmetry axis.[10] In this sense the lack of C_2 symmetry and the static configuration makes the (DMeDPQ)Pt and (BDPQ)Pt fragments excellent NMR probes of the ancillary bipy distortion. Despite the presence of many nuclei suitably positioned for magnetic monitoring of bipy distortion, we could not detect any ^{1}H or ^{13}C resonance splitting at 210 K for solutions of **1** and **2** (or for any of the other complexes studied here). This is a strong indication of planar bipy, which is not allowed to break the L-shaped molecular C_s symmetry. In agreement with this, the X-ray diffraction data of **1** show a perfectly planar Pt(bipy) skeleton. The disparity between the coordinated bipy geometry and fluxionality can be attributed to a slight but crucial difference in the orientation adopted, respectively by the *n*-Rpy of [Pt(bipy)(*n*-Rpy)$_2$]$^{2+}$, and quinoxaline pyridyl rings of **1** and **2**. Molecular models based on crystallographic data show, in fact, that the symmetrically disrotated quinoxaline pyridyl wings of [Pt(DMeDPQ)(bipy)]$^{2+}$ and [Pt(BDPQ)(bipy)]$^{2+}$ (rigid butterfly-like configuration) hamper, unlike the conrotated pyridine rings of [Pt(bipy)(*n*-Rpy)$_2$]$^{2+}$, twisting of the opposite bipy (Figure 2). Therefore, the bipy moieties of the L-shaped cations are forced into the same rigid planar structure as dppz and bdppz. Indeed, low-temperature NMR spectra of [Pt(dppz)(*n*-Rpy)$_2$]$^{2+}$ and [Pt(dppz)(*n*-Rpy)$_2$]$^{2+}$, as the L-shaped cations, do not show resonance splitting.[12]

The monodentate 3-substituted pyridines 3-Rpy are the ancillary ligands in **7**−**9**. In **9** we introduced a methyl substituent on the pyridine ring to gain clues concerning geometry and monitoring of the dynamics, as hindered rotation of 3-Mepy would lead to an NMR-detectable *s-cis*/*s-trans* rotamer equilibrium.[10] Solutions of **9** actually show resonances of a single compound. This could either mean a much greater thermodynamic stability of one rotamer, or a low rotational barrier for 3-Rpy (fast exchange). Very accurate selective NOED spectra indicate a spatial 2-H/6-H connectivity attributable to the neighbouring pyridine rings. This excludes the unique presence of an *s-cis* rotamer, but is consistent with both a static *s-trans* rotamer and fast rotation. Positive NOEs for **9** were also detected between the quinoxaline 6′-H and both 2-H and 6-H of the pyridyl moieties. Indeed, dipolar couplings by themselves suggest 3-Mepy rotation leading to transient 2-H/6-H contacts between nuclei of the neighbouring 3-Mepy; and also 2-H and 6-H temporarily alternate their proximity to 6′-H of the static quinoxaline pyridyl rings (Figure 3). This conclusion is further supported by the ^{13}C-^{1}H relaxation-time constants of **7** and **9**. Under decoupling conditions, for a pure dipolar relaxation in the extreme narrowing limit (neglect-

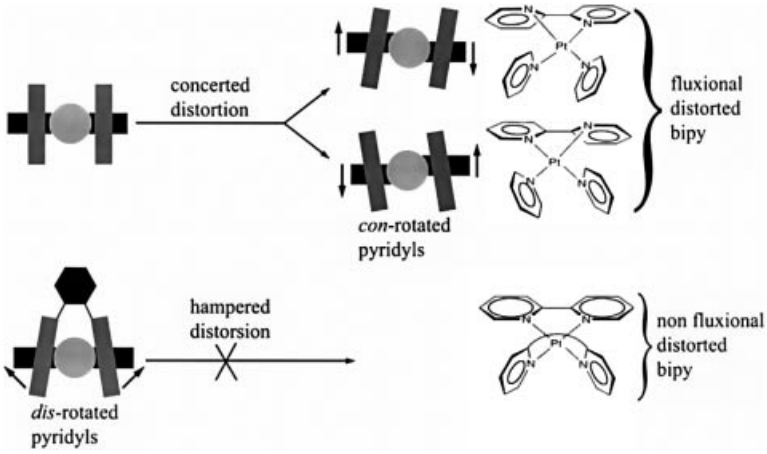

Figure 2. Allowed or hampered distortion of Pt(bipy) cations

ing contributions of unattached protons and considering the C−H distance to be constant), the aromatic ^{13}C-^{1}H relaxation time can be taken as a measure of the anisotropic spin diffusion.[13] The rotation of rings anchored to a bulk matrix slows down the relaxation rates of the *ortho*- and *meta*-carbon atoms without altering the *para*-carbon atom, whose proton-attached dependent local field is not affected by the rotational diffusion. The increased relaxation-time constants shown by the *ortho*- and *meta*-carbon atoms relative to the *para*-carbon atom are thus consistent with fast 3-Rpy rotation (Table 3).

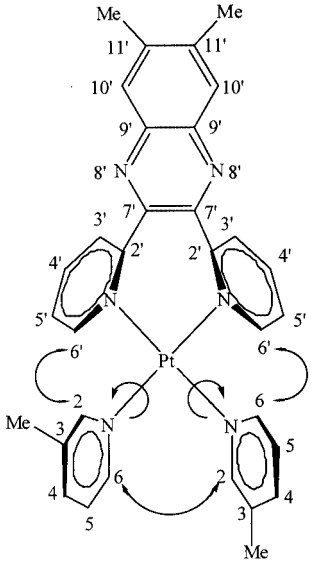

Figure 3. Remarkable dipolar couplings detected for **9** by NOESY NMR spectroscopy

The low-temperature NMR spectra of **9** in acetone at 210 K do not show evidence of 3-Mepy freezing, in agreement with a low rotational barrier of the pyridine ring. On the contrary, the corresponding $[Pt(bipy)(3\text{-}Mepy)_2]^{2+}$ cation shows *s-cis* and *s-trans* rotamers interconverting at 320 K with $\Delta G^{\#}$ of 68.5 kJ·mol^{-1}.[10] This difference can be attributed to the quasi-vertical orientation of quinoxaline

Table 3. Selected relaxation-time constants [s] of the aromatic ^{13}C-H carbon atoms in [D_6]acetone at 298 K; standard deviations are less than 5%

	DMeDPQ						3-Rpy			
	C-3′	C-4′	C-5′	C-6′	C10′	C-2	C-3	C-4	C-5	C-6
7	0.79	0.78	0.84	0.81	0.88	1.31	1.35	0.90	1.35	1.31
9	0.74	0.72	0.80	0.75	0.85	1.21	–	0.85	1.28	1.16

pyridyl rings which remove hindrance from the coordination plane. Analogous conclusions can be drawn from the NMR spectra of **7** and **8** showing, also at 210 K, three pyridine resonances (for the four *ortho*, four *meta* and two *para* nuclei, respectively) due to symmetry averaging about the coordination plane prompted by fast pyridine rotation.

Despite all our efforts we were not able to prepare 2-Mepy quinoxaline complexes. It is likely that coordination is inhibited by the steric hindrance between the *ortho*-methyl substituent and the hetroaromatic rings.

Molecular Structure of {[Pt(DMeDPQ)(bipy)][PF_6]$_2$}·0.5{(DMeDPQ)(CH_3OH)}

The 6,7-dimethyl-2,3-bis(2-pyridyl)quinoxaline ligand (DMeDPQ) crystallises with the platinum salt in a 3:2 ratio. The crystal contains a discrete complex $[Pt(DMeDPQ)(bipy)]^{2+}$ cation with the hexafluorophosphate ions as counterions (ratio 1:2), and co-crystallised uncoordinated ligand and methanol solvent (both in a 2:1 ratio). This solid-state aggregate is stabilized by strong π-stacking (3.6 Å) between the planar quinoxaline fragment of the alternate free and coordinated ligands along the *c* axis: the anions and the methanol molecules are retained between these parallel columns by hydrogen-bonding interactions. The 3-D packing arrangement is very ordered and shows an overall symmetry (expressed by the adopted crystallographic space group) higher than the single compound moieties, which causes an important symmetry disorder for the free ligand and one PF_6^- anion.

The coordinated quinoxaline ligand shows the same arrangement as adopted in a previous Pd compound [$PdCl_2$(DMeDPQ)][6] showing a slight conjugation between the aromatic bicyclic system and the pyridine ring, as evidenced by the N2−C10−C11−C11′ torsion angles [−52.9(5)° vs. the average value of 57.5(4)°] that is similar to the corresponding value in the free disordered ligand [−48(1)°]. This typical butterfly arrangement, which allows the nitrogen lone pairs to be oriented out of the ligand plane towards the metal atom in the coordinated quinoxaline, is also observed in the uncoordinated ligand.[14] The steric requirements of the ligand bite may also be responsible for the significant deformations from planarity of the quinoxaline[15] and the enlargement of the pyridine substituent angles up to 130° (protonated free ligand).[16]

The pyridyl orientation causes the quinoxaline mean plane to be normal to the platinum coordination plane containing the bipyridyl ligand, with a dihedral angle between them of 81.09(9)°. The angle of 71.4(2)° between the quinoxaline pyridine rings and the Pt coordination plane may indicate a possible interaction of the π-orbitals of both rings with the d_{xz}, d_{yz} and d_{xy} orbitals of the metal atom.[17] The DMeDPQ and bipy Pt−N bond lengths are similar [2.027(4) vs. 2.013(3) Å, respectively], the angular distortion from the regular square-planar Pt coordination geometry being mainly due to the different bite size of the two ligands (Figure 4).

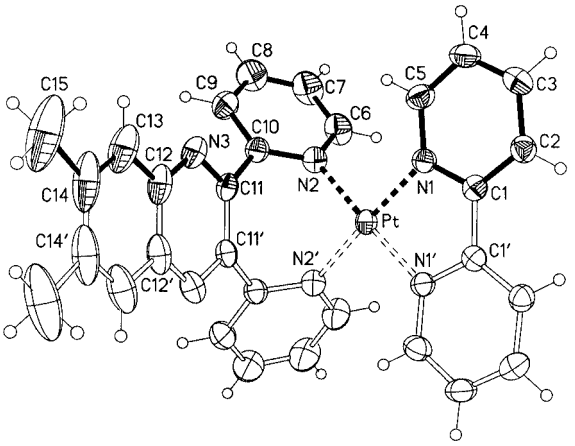

Figure 4. View of the cation of complex **1**, which lies on a mirror plane, with its labelling scheme; empty atoms represent the symmetric half moiety generated by the $x, -y + 1, z$ operation; anions, co-crystallised uncoordinated ligand and methanol moieties have been omitted for clarity; thermal ellipsoids are drawn at 30% probability while the hydrogen-atom size is arbitrary; selected bond lengths [Å] and angles [°]: Pt−N1 2.013(3), Pt−N2 2.027(4), N1−C1 1.365(5), C1−C1′ 1.457(8), N2−C10 1.341(5), C10−C11 1.480(6), C11−C11′ 1.425(9), C11−N3 1.330(5), N3−C12 1.368(6), C12−C12′ 1.42(1); N1−Pt−N2 97.0(1), N1′−Pt−N1 80.7(2), N2−Pt−N2′ 85.2(2), N1−C1−C1′ 114.9(2), C2−C1−C1′ 124.3(3), N3−C11−C10 113.4(4), C11′−C11−C10 124.9(2)

Conclusions

Quinoxalines lead to L-shaped Pt^{II} complexes of C_s local symmetry. The rigid butterfly-like structure gives these complexes stereochemical properties, which can be exploited for studying geometry and fluxionality of several ancillary ligands. The prochiral character of coordinated quinoxaline could pave the way to enantioselective synthesis and new classes of chiral compounds.

Experimental Section

General Remarks: ^1H and $^{13}C\{^1H\}$ NMR spectra were recorded with a Bruker ARX 300 spectrometer, at 300.13 and 75.47 MHz, respectively. The ^1H NMR spectra were calibrated against the residual proton signals of the solvent as internal reference ([D_6]acetone, δ = 2.04 ppm), the $^{13}C\{^1H\}$ spectra were calibrated against the septuplet signals of the solvent ([D_6]acetone δ = 29.80 ppm).

Synthesis: Complexes **1** and **2** were prepared by dissolving DMeDPQ (Aldrich) or BDPQ[18] (2.5 mmol), respectively, in 100 mL of CH_3OH, adding H_2O to give a 1:1 CH_3OH/H_2O mixture and suspending a slight excess (5%) of [$PtCl_2$(bipy)][19] with respect to the stoichiometric ratio in it. The mixture was then heated to boiling and kept refluxing for 1/2 h until almost complete dissolution of the platinum complex. After filtration to eliminate the traces of solid material, NH_4PF_6 was added and the resulting complexes **1** and **2** precipitated as yellow solids, which were recrystallised from CH_3OH. Yields: 75% (**1**), 83% (**2**).

Complexes **3**−**6** were synthesised starting from the corresponding phenazine (dppz[20] or bdppz[21]) dichloride, obtained as follows: The phenazine ligand (2.5 mmol) was dissolved in 100 mL of warm (ca. 50 °C) DMSO and added dropwise and with stirring to an equivalent amount of [$PtCl_2(DMSO)_2$],[22] also dissolved in 100 mL of warm DMSO. After a few minutes, the red (phenazine)platinum dichloride, initially yellow in the case of [$PtCl_2$(dppz)], precipitated. To facilitate its coagulation, the mixture was stirred for 1 h, then filtered, washed with H_2O and a few drops of CH_3OH to eliminate the DMSO, and air-dried. A slight excess of the dichloride thus obtained was then suspended in a CH_3OH/H_2O (2:1) mixture (300 mL) in which the quinoxaline ligand (DMeDPQ or BDPQ; 2.5 mmol) had been previously dissolved. To facilitate the dissolution of the sparingly soluble phenazine dichloride complex, a few drops of DMSO were added and the mixture was heated to boiling and kept refluxing for 3 d. After cooling, insoluble material was separated by centrifugation, and the final product precipitated from the coloured solution (yellow for the complexes with dppz and orange-red for the ones with bdppz) by addition of an excess of NH_4PF_6. Since the yield of the reaction was very low, especially for the two complexes with bdppz, it was necessary to recover the unchanged (dppz)- and (bdppz)platinum dichloride from the bottom of the test tubes, and to repeat 2−3 times, under the same conditions, the treatment with the corresponding quinoxaline ligand. The ivory [Pt(DMeDPQ)(dppz)]$(PF_6)_2$, the reddish [Pt(DMeDPQ)(bdppz)]$(PF_6)_2$, the orange-brown [Pt(BDPQ)(dppz)]$(PF_6)_2$ and the brick-red [Pt(BDPQ)(bdppz)]$(PF_6)_2$ were all recrystallised from CH_3CN. Yields: 61% (**3**), 27% (**4**), 69% (**5**), 20% (**6**).

For the synthesis of complexes **7**−**9** it was necessary to prepare the corresponding (DMeDPQ)- or (BDPQ)platinum dichloride. To this end, the quinoxaline ligand (2.5 mmol) was dissolved in warm (ca. 50 °C) DMSO (100 mL) and added dropwise with stirring to an equivalent amount of [$PtCl_2(DMSO)_2$],[22] also dissolved in DMSO (100 mL). After a few minutes, an off-white product, in the case of [$PtCl_2$(DMeDPQ)], or a deep yellow one, for [$PtCl_2$(BDPQ)],

precipitated. Since the chloro complexes were very powdery and so very difficult to filter, after 5 h a few drops of H_2O were added to facilitate their coagulation and then filtered through a water pump. The product was washed with H_2O and a few drops of CH_3OH to eliminate the DMSO, and air-dried. The dichloride complex thus obtained was then suspended in H_2O in the presence of the appropriate pyridine (5% excess with respect to the stoichiometric 1:2 ratio) and heated to boiling. After dissolution of the complex, NH_4PF_6 was added and the resulting complexes **7**−**9** precipitated as light-yellow solids, which were washed with H_2O and a few drops of CH_3OH, and air-dried. The complexes were then recrystallised from CH_3OH. Yields: 67% (**7**), 70% (**8**), 68% (**9**).

All complexes were characterised by elemental analysis and ^1H and ^{13}C NMR spectroscopy (see Scheme 3 for atom numbering). The structure of $[Pt(DMeDPQ)(bipy)][PF_6)_2$ was determined by a single-crystal X-ray analysis of $\{[Pt(DMeDPQ)(bipy)][PF_6]_2\}\cdot 0.5\{(DMeDPQ)(CH_4O)\}$.

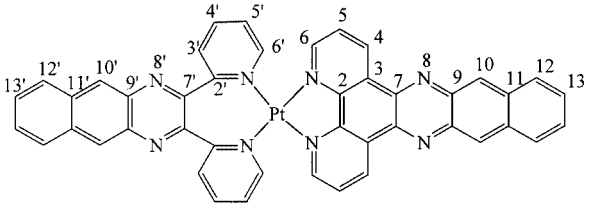

Scheme 3. General numbering scheme

[Pt(DMeDPQ)(bipy)](PF$_6$)$_2$ (1): ^1H NMR (300 MHz, [D$_6$]acetone): δ = 9.46 (d, ^3J = 5 Hz, 2 H, 6′-H), 8.67 (d, ^3J = 6 Hz, 2 H, 3-H), 8.57 (td, ^3J = 7, ^4J = 1 Hz, 2 H, 4′-H), 8.53 (td, ^3J = 7, ^4J = 1 Hz, 2 H, 4-H), 8.29 (d, ^3J = 6 Hz, 2 H, 3′-H), 8.18 (d, ^3J = 8 Hz, 2 H, 6-H), 8.14 (m, 2 H, 5′-H), 8.05 (s, 2 H, 10′-H), 7.83 (td, ^3J = 6, ^4J = 1 Hz 2 H, 5-H), 2.58 (s, 6 H, 12′-H) ppm. $^{13}C\{^1H\}$ NMR (75 MHz, [D$_6$]acetone): δ = 158.8 (2 C, C-2′), 157.5 (2 C, C-2), 153.2 (2 CH, C-6′), 150.9 (2 CH, C-6), 147.4 (2 C, C-7′), 145.2 (2 C, C-9′), 143.9 (2 CH, C-4′), 143.7 (2 CH, C-4), 141.5 (2 C, C-11′), 131.0 (2 CH, C-3′), 130.2 (2 CH, C-5′), 129.8 (2 CH, C-5), 129.2 (2 CH, C-10′), 125.6 (2 CH, C-3), 20.4 (2 CH$_3$, C-12′) ppm. $C_{30}H_{24}F_{12}N_6P_2Pt$ (954): calcd. C 37.79, H 2.54, N 8.81; found C 37.70, H 2.58, N 8.88.

[Pt(BDPQ)(bipy)](PF$_6$)$_2$ (2): ^1H NMR (300 MHz, [D$_6$]acetone): δ = 9.52 (d, ^3J = 5 Hz, 2 H, 6′-H), 8.98 (s, 2 H, 10′-H), 8.65 (d, ^3J = 8 Hz, 2 H, 3-H), 8.61 (td, ^3J = 7, ^4J = 1 Hz, 2 H, 4′-H), 8.53 (td, ^3J = 7, ^4J = 1 Hz, 2 H, 4-H), 8.39 (d, ^3J = 7 Hz, 2 H, 3′-H), 8.34 (m, 2 H, 12′-H), 8.22 (d, ^3J = 6 Hz, 2 H, 6-H), 8.18 (m, 2 H, 5′-H), 7.85 (m, 2 H, 5-H), 7.78 (m, 2 H, 13′-H) ppm. $^{13}C\{^1H\}$ NMR (75 MHz, [D$_6$]acetone): δ = 158.6 (2 C, C-2′), 157.6 (2 C, C-2), 153.3 (2 CH, C-6′), 150.9 (2 CH, C-6), 148.7 (2 C, C-7′), 144.0 (2 CH, C-4′), 143.9 (2 CH, C-4), 138.4 (2 C, C-9′), 136.2 (2 C, C-11′), 131.3 (2 CH, C-3′), 130.4 (2 CH, C-5′), 129.8 (2 CH, C-5), 129.6 (2 CH, C-10′), 129.4 (4 CH, C-13′, C-12′), 125.6 (2 CH, C-3) ppm. $C_{32}H_{22}F_{12}N_6P_2Pt$ (976): calcd. C 39.40, H 2.27, N 8.61; found C 39.21, H 2.38, N 8.56.

[Pt(DMeDPQ)(dppz)](PF$_6$)$_2$ (3): ^1H NMR (300 MHz, [D$_6$]acetone): δ = 10.01 (dd, ^3J = 8, ^4J = 1 Hz, 2 H, 4-H), 9.60 (d, ^3J = 6 Hz, 2 H, 6′-H), 8.71 (dd, ^3J = 5, ^4J = 1 Hz, 2 H, 6-H), 8.63 (td, ^3J = 8, ^4J = 1 Hz, 2 H, 4′-H), 8.47 (m, 2 H, 10-H), 8.36 (m, 2 H, 3′-H), 8.33 (dd, ^3J = 8, ^3J = 5 Hz, 2 H, 5-H), 8.21 (m, 4 H, 5′-H and 11-H), 8.05 (s, 2 H, 10′-H), 2.54 (s, 6 H, Me) ppm. $^{13}C\{^1H\}$ NMR (75 MHz, [D$_6$]acetone): δ = 159.0 (2 C, C-2′), 153.4 (2 CH, C-6′), 152.9 (2 CH, C-6), 151.1 (2 C, C-2), 147.6 (2 C, C-7′), 145.5 (2 C, C-9′), 143.9 (2 CH, C-4′), 143.7 (2 C, C-7), 141.4 (2 C, C-11′), 139.6 (2 C, C-9), 139.5 (2 CH, C-4), 134.0 (2 CH, C-11), 131.7 (2 C, C-3), 131.2 (2 CH, C-3′) 130.6 (2 CH, C-10) 130.3 (2 CH, C-5′), 129.3 (2 CH, C-5), 129.2 (2 CH, C-10′), 20.4 (2CH3, C-12′) ppm. $C_{38}H_{26}F_{12}N_8P_2Pt$ (1080): calcd. C 42.27, H 2.43, N 10.38; found C 42.13, H 2.45, N 10.26.

[Pt(DMeDPQ)(bdppz)](PF$_6$)$_2$ (4): ^1H NMR (300 MHz, [D$_6$]acetone): δ = 9.88 (d, ^3J = 9 Hz, 2 H, 4-H), 9.62 (d, ^3J = 5 Hz, 2 H, 6′-H), 8.92 (s, 2 H, 10-H), 8.65 (m overlapped, 4 H, 6-H and 4′-H), 8.39 (m, 2 H, 3′-H), 8.29 (m, 2 H, 5-H), 8.23 (m, 2 H, 5′-H), 8.14 (m, 2 H, 12-H), 8.09 (s, 2 H, 10′-H), 7.55 (m, 2 H, 13-H), 2.54 (s, 6 H, 12′-H) ppm. $^{13}C\{^1H\}$ NMR (75 MHz, [D$_6$]acetone): δ = 159.0 (2 C, C-2′), 153.5 (2 CH, C-6′), 152.9 (2 CH, C-6), 151.5 (2 C, C-2), 147.6 (2 C, C-7′), 145.6 (2 C, C-9′), 144.0 (2 CH, C-4′), 141.4 (2 C, C-11′), 140.0 (2 C, C-7), 139.4 (2 CH, C-4), 139.1 (2 C, C-9), 136.0 (2 C, C-11), 131.8 (2 CH, C-3), 131.2 (2 CH, C-3′), 130.4 (2 CH, C-5′), 129.6 (2 CH, C-5), 129.3 (2 CH, C-12, C-13), 129.2 (2 CH, C-10), 129.1 (2 CH, C-10′), 20.4 (2CH$_3$, C-12′) ppm. $C_{42}H_{28}F_{12}N_8P_2Pt$ (1130): calcd. C 44.65, H 2.50, N 9.92; found C 44.47, H 2.56, N 9.88.

[Pt(BDPQ)(dppz)](PF$_6$)$_2$ (5): ^1H NMR (300 MHz, [D$_6$]acetone): δ = 9.99 (dd, ^3J = 8, ^4J = 1 Hz, 2 H, 4-H), 9.65 (d, ^3J = 5 Hz, 2 H, 6′-H), 8.96 (s, 2 H, 10′-H), 8.73 (td, ^3J = 6, ^4J = 1 Hz, 2 H, 6-H), 8.66 (td, ^3J = 8, ^4J = 1 Hz, 2 H, 4′-H), 8.44 (m, overlapped 4 H, 3′-H and 10-H), 8.33 (m, 2 H, 5-H), 8.31 (m, 2 H, 12′-H), 8.29 (m, 2 H, 5′-H), 8.17 (dd, ^3J = 6, ^4J = 3 Hz, 2 H, 11-H), 7.73 (dd, ^3J = 6, ^4J = 3 Hz, 2 H, 13′-H) ppm. $^{13}C\{^1H\}$ NMR (75 MHz, [D$_6$]acetone): δ = 158.8 (2 C, C-2′), 153.5 (2 CH, C-6′), 152.9 (2 CH, C-6), 151.1 (2 C, C-2), 148.6 (2 C, C-7′) 144.1 (2 CH, C-4′), 143.7 (2 C, C-7), 139.6 (2 C, C-9), 139.5 (2 CH, C-4), 138.3 (2 C, C-9′), 136.2 (2 C, C-11′), 134.0 (2 CH, C-11), 131.6 (2 C, C-3), 131.4 (2 CH, C-3′), 130.6 (4 CH, C-10, C-5′), 129.5 (2 CH, C-5), 129.4 (2 CH, C-13′), 129.3 (4 CH, C-10′, C-12′) ppm. $C_{40}H_{24}F_{12}N_8P_2Pt$ (1102): calcd. C 43.61, H 2.20, N 10.17; found C 43.65, H 2.11, N 10.07.

[Pt(BDPQ)(bdppz)](PF$_6$)$_2$ (6): ^1H NMR (300 MHz, [D$_6$]acetone): δ = 9.86 (d, ^3J = 9 Hz, 2 H, 4-H), 9.67 (d, ^3J = 5 Hz, 2 H, 6′-H), 9.00 (s, 2 H, 10′-H), 8.88 (s, 2 H, 10-H), 8.68 (m, 2 H, 4′-H), 8.66 (d, ^3J = 6 Hz, 2 H, 6-H), 8.48 (d, ^3J = 9 Hz, 2 H, 3′-H), 8.29 (overlapped m, 6 H, 5-H, 5′-H, 12′-H), 8.11 (m, 2 H, 12-H), 7.71 (dd, ^3J = 6, ^4J = 3 Hz, 2 H, 13′-H), 7.52 (dd, ^3J = 6, ^4J = 3 Hz, 2 H, 13-H) ppm. $^{13}C\{^1H\}$ NMR (75 MHz, [D$_6$]acetone): δ = 158.8 (2 C, C-2′), 153.6 (2 CH, C-6′), 152.9 (2 CH, C-6), 151.4 (2 C, C-2), 148.6 (2 CH, C-7′), 144.1 (2 CH, C-4′), 140.0 (2 C, C-7), 139.4 (2 CH, C-4), 139.1 (2 C, C-9), 138.4 (2 C, C-9′), 136.2 (2 C, C-11′), 135.9 (2 C, C-11), 131.8 (2 C, C-3), 131.5 (2 CH, C-3′), 130.6 (2 CH, C-5′), 129.5 (6 CH, C-5, C-10′, C-12′), 129.4 (2 CH, C-13′), 129.3 (4 CH, C-10, C-12), 129.1 (2 CH, C-13) ppm. $C_{44}H_{26}F_{12}N_8P_2Pt$ (1152): calcd. C 45.88, H 2.28, N 9.73; found C 45.81, H 2.22, N 9.65.

[Pt(DMeDPQ)(py)$_2$](PF$_6$)$_2$ (7): ^1H NMR (300 MHz, [D$_6$]acetone): δ = 9.24 (d, ^3J = 6 Hz, 2 H, 6′-H), 8.92 (dd, ^3J = 7, ^4J = 2 Hz, 4 H, 2-H = 6-H), 8.37 (td, ^3J = 8, ^4J = 1 Hz, 2 H, 4′-H), 8.21 (dd, ^3J = 7, ^4J = 1 Hz, 2 H, 3′-H), 8.19 (s, 2 H, 10′-H), 8.07 (tt, ^3J = 7, ^4J = 2 Hz, 2 H, 4-H), 7.86 (td, ^3J = 8, ^4J = 1 Hz, 2 H, 5′-H), 7.62 (m, 4 H, 3-H = 5-H), 2.70 (s, 6 H, 12′-H). $^{13}C\{^1H\}$ NMR (75 MHz, [D$_6$]acetone): δ = 158.6 (2 C, C-2′), 152.7 (4 CH, C-2 = C-6), 152.1 (2 CH, C-6′), 147.6 (2 C, C-7′), 145.2 (2 C, C-9′), 143.2 (2 CH, C-4′), 142.5 (2 CH, C-4), 141.9 (2 C, C-11′), 130.9 (2 CH,

C-3′), 129.5 (2 CH, C-10′), 128.9 (2 CH, C-5′), 128.8 (4 CH, C-3 to C-5), 20.6 (2 CH_3) ppm. $C_{30}H_{26}F_{12}N_6P_2Pt$ (956): calcd. C 37.71, H 2.74, N 8.79; found C 37.66, H 2.89, N 8.67.

[Pt(BDPQ)(py)$_2$](PF$_6$)$_2$ (8): ^{1}H NMR (300 MHz, [D$_6$]acetone): δ = 9.29 (d, ^3J = 6 Hz, 2 H, 6′-H), 9.12 (s, 2 H, 10′-H), 8.94 (dd, ^3J = 7, ^4J = 2 Hz, 4 H, 2-H = 6-H), 8.46 (dd, ^3J = 6, ^4J = 3 Hz, 2 H, 12′-H), 8.40 (dd, ^3J = 8, ^4J = 2 Hz, 2 H, 4′-H), 8.31 (dd, ^3J = 7, ^4J = 1 Hz, 2 H, 3′-H), 8.07 (m, 2 H, 4-H), 7.91 (m, 2 H, 5′-H), 7.88 (dd partially overlapped with 5′-H, ^3J = 6, ^4J = 3 Hz, 2 H, 13′-H), 7.62 (dd, ^3J = 7, ^4J = 2 Hz, 4 H, 3-H = 5-H) ppm. $^{13}C\{^1H\}$ NMR (75 MHz, [D$_6$]acetone): δ = 158.5 (2 C, C-2′), 152.7 (4 CH, C-2−C-6), 152.3 (2 CH, C-6′), 148.7 (2 C, C-7′), 143.4 (2 CH, C-4′), 142.6 (2 CH, C-4), 138.9 (2 C, C-9′), 136.3 (2 C, C-11′), 131.1 (2 CH, C-3′), 129.7 (4 CH, C-10′, C-12′), 129.4 (2 CH, C-13′), 129.1 (2 CH, C-5′), 128.8 (4 CH, C-3 = C-5) ppm. $C_{32}H_{24}F_{12}N_6P_2Pt$ (978): calcd. C 39.32, H 2.47, N 8.58; found C 39.17, H 2.41, N 8.67.

[Pt(DMeDPQ)(3-Mepy)$_2$](PF$_6$)$_2$ (9): ^{1}H NMR (300 MHz, [D$_6$]acetone): δ = 9.22 (d, ^3J = 6 Hz, 2 H, 6′-H), 8.80 (s, 2 H, 2-H), 8.71 (d, ^3J = 6 Hz, 2 H, 6-H), 8.35 (td, ^3J = 8, ^4J = 1 Hz, 2 H, 4′-H), 8.19 (m overlapped, 4 H, 10′-H and 3′-H), 7.86 (m overlapped, 4 H, 4-H and 5′-H), 7.47 (dd, ^3J = 8, ^3J = 6 Hz, 2 H, H- 5), 2.70 (s, 6 H, 12′-H), 2.26 (s, 6 H, 3-Me) ppm. $^{13}C\{^1H\}$ NMR (75 MHz, [D$_6$]acetone): δ = 158.3 (2 C, C-2′), 152.0 (2 CH, C-2), 151.8 (2 CH, C-6′), 149.5 (2 CH, C-6) 147.5 (2 C, C-7′), 145.2 (2 C, C-9′), 142.9 (2 CH, C-4′), 142.6 (2 CH, C-4), 141.8 (2 C, C-11′), 139.2 (2 C, C-3), 130.5 (2 CH, C-3′), 129.3 (2 CH, C-10′), 128.5 (2 CH, C-5′), 127.7 (2 CH, C-5), 20.2 (2 CH_3, C-12′), 17.9 (2 CH_3, 3-Mepy) ppm. $C_{32}H_{30}F_{12}N_6P_2Pt$ (984): calcd. C 39.07, H 3.07, N 8.54; found C 39.16, H 2.99, N 8.67.

X-ray Crystallographic Study of [Pt(DMeDPQ)(bipy)](PF$_6$)$_2$·0.5{(C$_{20}$H$_{16}$N$_4$)(CH$_4$O)}: Suitable crystals of the title complex were obtained by slow solvent evaporation from a methanol solution of **1**. Diffraction data were collected with a Siemens P4 automatic four-circle diffractometer. A summary of the crystallographic data and the structure refinement is reported in Table 4. No crystal deterioration was evidenced by monitoring of three standard reflection measurements. The reflection intensities were evaluated by a learnt-profile procedure[23] among 2θ shells and then corrected for Lorentz-polarisation effects. Absorption correction was applied by fitting a pseudo-ellipsoid to the azimuthal scan data (0−360° range by a 10° step) of 15 high reflections.[24] Data collection and reduction were performed with the SHELXTL[25] package. The diffraction data did not allow us to determine uniquely the crystal packing symmetry and the structure modellisation was carried out in all the three possible monoclinic space groups *C*2, *Cm* and *C*2/*m*. The refinement in the two acentric space groups was seriously hampered by several very strong parameter correlations (> 0.9) while the centrosymmetric one shows incompatibility between the crystallographic point symmetries and the compound moieties in special positions. The structure was solved in *C*2/*m* by a combination of standard direct methods[26] and Fourier synthesis, and refined by minimizing the function $\Sigma w(F_o^2 - F_c^2)^2$ with the full-matrix least-squares technique based on all independent *F*, with SHELXL-97.[27] All non-hydrogen atoms were refined anisotropically. Hydrogen atoms were included in the model refinement with the "riding model" method with the X−H bond geometry and isotropic displacement parameter depending on the parent atom X. The co-crystallised methanol and uncoordinated quinoxaline molecules were placed in crystallographic special positions having a higher symmetry than these molecules. This generates a significant symmetry disorder. Further, one hexafluorophosphate anion shows the usual rotational disorder evidenced by the overlap of two symmetric orientations related by the intersecting mirror plane. All attempts to represent the biggest ellipsoids as adjacent atomic partial occupancies were unsuccessful. The final geometrical calculations and drawings were carried out with the PARST program[28] and the XPW utility of the Siemens package, respectively. CCDC-237593 contains the supplementary crystallographic data for this paper. These data can be obtained free of charge at www.ccdc.cam.ac.uk/conts/retrieving.html [or from the Cambridge Crystallographic Data Centre, 12 Union Road, Cambridge CB2 1EZ, UK; Fax: + 44-1223-336-033; E-mail: deposit@ccdc.cam.ac.uk].

Table 4. Crystallographic data for **1**

Empirical formula	{[$C_{30}H_{24}N_6Pt$][PF_6]$_2$}·0.5{($C_{20}H_{16}N_4$)(CH_4O)}
Formula mass	1125.79
Crystal size	0.32 × 0.25 × 0.19 mm
Crystal colour, form	yellow, irregular
Crystal system	monoclinic
Space group	*C*2/*m* (no. 12)
Unit cell dimensions	*a* = 30.431(5) Å
	b = 12.637(2) Å
	c = 11.923(2) Å
	β = 90.84(1)°
V	4585(1) Å^3
Z	4
F(000)	2212
ρ_{calcd}	1.631 g/cm^3
μ	3.219 mm^{-1}
λ (graphite-monochromated)	0.71073 Å (Mo-K_α)
2Θ range	4.3−54°
No. of data collected (2θ-ω)	5294
No. of data independent (refined)	5197 (R_{int} = 0.0214)
No. of data observed	3931 [$I \geq 2\sigma(I)$]
No. of variables	344
Completeness to 2θ = 50°	0.987%
*R*1[a] (observed/refined data)[a]	0.0353/0.0782
*wR*2[b] (observed/refined data)	0.0544/0.0822
GOF[c] (observed/refined data)	0.951/0.951
Max. diff. peak and hole	0.752/−0.555 e·Å^{-3}
Max. and mean shift/esd	0.007/0.001

[a] $R = [\Sigma||F_o| - |F_c||]/\Sigma|F_o|$. [b] $R_w = \{\Sigma[w(F_o^2 - F_c^2)^2]/[\Sigma w(F_o^2)^2]\}^{1/2}$. [c] GOF = $\{\Sigma[w(F_o^2 - F_c^2)^2/(N_{obs} - N_{var})]\}^{1/2}$.

[1] A. Escuer, R. Vicente, T. Comas, J. Ribas, M. Gomez, X. Solans, D. Gatteschi, C. Zanchini, *Inorg. Chim. Acta* **1991**, *181*, 51−60.
[2] K. C. Gordon, A. H. R. Al-Obaidi, P. M. Jayaweera, J. J. McGarvey, J. F. Malone, S. E. J. Bell, *J. Chem. Soc., Dalton Trans.* **1996**, 1591−1596.
[3] A. Escuer, T. Comas, J. Ribas, R. Vicente, X. Solans, C. Zanchini, D. Gatteschi, *Inorg. Chim. Acta* **1989**, *162*, 97−103.
[4] G. Bandoli, T. I. A. Gerber, R. Jacobs, J. G. H. du Preez, *Inorg. Chem.* **1994**, *33*, 178−179.
[5] K. V. Goodwin, W. T. Pennington, J. D. Petersen, *Acta Crystallogr., Sect. C* **1990**, *46*, 898−900.
[6] F. Nicolò, M. Cusumano, M. L. Di Pietro, R. Scopelliti, G. Bruno, *Acta Crystallogr., Sect. C* **1998**, *54*, 485−487.
[7] M. Cusumano, M. L. Di Pietro, A. Giannetto, F. Nicolò, B. Nordén, P. Lincoln, *Inorg. Chem.* **2004**, *43*, 2416−2421.
[8] J. Granifo, M. E. Vargas, H. Rocha, M. T. Garland, R. Baggio, *Inorg. Chim. Acta* **2001**, *321*, 209−214.

[9] J. Granifo, M. T. Garland, R. Baggio, *Inorg. Chim. Acta* **2003**, *348*, 263−270.
[10] E. Rotondo, G. Bruschetta, G. Bruno, A. Rotondo, M. L. Di Pietro, M. Cusumano, *Eur. J. Inorg. Chem.* **2003**, 2612−2618.
[11] [11a] Z. Qin, M. C. Jennings, R. J. Puddephatt, *Chem. Commun.* **2001**, 2676−2677. [11b] H.-Q. Liu, S.-M. Peng, C. M. Che, *J. Chem. Soc., Chem. Commun.* **1995**, 509−510.
[12] E. Rotondo, unpublished results.
[13] [13a] G. C. Levy, *J. Chem. Soc., Chem. Commun.* **1972**, 47−48. [13b] M. Fuss, H. U. Siehl, B. Olenyuk, P. J. Stang, *Organometallics* **1999**, *18*, 758−769.
[14] K. Wozniak, *Acta Crystallogr., Sect. C* **1991**, *47*, 1761−1763.
[15] S. C. Rasmussen, M. M. Richter, E. Yi, H. Place, K. J. Brewer, *Inorg. Chem.* **1990**, *29*, 3926−3932.
[16] K. Wozniak, T. M. Krygowski, E. Grech, *Pol. J. Chem.* **1994**, *68*, 1813−1817.
[17] A. Albinati, C. Arz, P. S. Pregosin, *Inorg. Chem.* **1987**, *26*, 508−513.
[18] L. M. Vogler, C. Franco, S. W. Jones, K. J. Brewer, *Inorg. Chim. Acta* **1994**, *221*, 55−59.
[19] G. T. Morgan, F. H. Burstall, *J. Chem. Soc.* **1934**, 965−971.
[20] J. E. Dickenson, L. A. Summers, *Aust. J. Chem.* **1970**, *23*, 1023−1027.
[21] P. Lincoln, A. Broo, B. Nordén, *J. Am. Chem. Soc.* **1996**, *118*, 2644−2653.
[22] Yu. N. Kukushkin, Yu. E. Vyaz′menskii, L. J. Zorina, Yu. L. Pazukhina, *Russ. J. Inorg. Chem.* **1968**, *13*, 1595−1599; *Chem. Abstr.* **1968**, *69*, 40851j.
[23] R. Diamond, *Acta Crystallogr., Sect. A* **1969**, *25*, 43−55.
[24] G. Kopfmann, R. Huber, *Acta Crystallogr., Sect. A* **1968**, *24*, 348−351.
[25] G. M. Sheldrick, *SHELXTL*, VMS version 5.05, Siemens Analytical X-ray Instruments Inc., Madison, Wisconsin, **1991**.
[26] A. Altomare, O. Cascarano, C. Giacovazzo, A. Guagliardi, M. C. Burla, G. Polidori, M. Camalli, *J. Appl. Crystallogr.* **1994**, *27*, 435−436.
[27] G. M. Sheldrick, *SHELXL-97, Program for Crystal Structure Refinement*, University of Göttingen, Germany, **1997**.
[28] M. Nardelli, *J. Appl. Chem.* **1995**, *28*, 659; locally modified version).

Received May 20, 2004
Early View Article
Published Online October 26, 2004

